Compact, digital and self-powered piezoelectric vibration energy harvester with generation control using voltage measurement circuit

著者	Yushin Hara, Kensuke Saito, Kanjuro Makihara
journal or publication title	Sensors and Actuators A: Physical
volume	299
page range	111609
year	2019-11-01
URL	http://hdl.handle.net/10097/00133307

doi: 10.1016/j.sna.2019.111609

This is the accepted version of the following article:

Hara, Y., Saito, K., and Makihara, K., "Compact, Digital and Self-Powered Piezoelectric Vibration Energy Harvester with Generation Control using Voltage Measurement Circuit," Sensors & Actuators: A. Physical, Vol. 299, 1, 2019, Article No. 111609. (DOI: 10.1016/j.sna.2019.111609)

Compact, digital and self-powered piezoelectric vibration energy harvester with generation control using voltage measurement circuit

Yushin Hara*, Kensuke Saito, Kanjuro Makihara**

Department of Aerospace Engineering, Tohoku University, 6-6-1, Aoba, Aramaki, Aoba-ku, Sendai 980-8578, Japan

* Corresponding author. E-mail address: hara@ssl.mech.tohoku.ac.jp (Y. Hara)

** Coauthor E-mail address: makihara@ssl.mech.tohoku.ac.jp (K. Makihara)

Abstract

As piezoelectric vibration energy harvesting (PVEH) extracts electrical energy from vibration, it is a promising portable power device. Although harvesting efficiency can be increased by using switch controls based on vibration displacement, such controls require external controllers and sensors, which consume energy and occupy space in a device. To separate external energy sources and sensors from a switch controller, we propose a measurement circuit and a digital controller for PVEH to increase autonomy, flexibility, and compactness. In the present study, switch controls are realized on a self-powered digital controller using the piezoelectric voltage as an observation value, where achieves a switch-controlled PVEH independent from additional external sensors. We discuss the characteristics of the proposed circuit and evaluate the harvesting performance. The experimental results demonstrated that the proposed sensor-less harvester has a harvesting performance comparable to that of a conventional sensor-equipped harvester.

Keywords: Vibration energy harvesting, Piezoelectric system, Self-powered device, Digital control

Notation

b_p	Piezoelectric coefficient	R_{load}	Device resistance
C_p	Transducer capacitance	r	Resistance of inductor and electric circuit
C_S	Battery capacitance	S	Switch
D_i	Diode element (i = 1 to 4)	V_p	Voltage generated by piezoelectric transducer
L	Inductance	V_{load}	Voltage of device resistance
P_{load}	Load energy consumption	V_{pos}	Measured signal on positive side
Q	Electric charge in the piezoelectric transducer	V_{neg}	Measured signal on negative side
Q_{before}	Piezoelectric charge before switching	V_{mes}	Measured voltage by the proposed circuit
Q_{after}	Piezoelectric charge after switching	x_s	Displacement during switch control
R_j	Resistance of measurement circuit (j = 1 to 6)	x	Displacement of piezoelectric transducer

1. Introduction

Piezoelectric vibration energy harvesting (PVEH) converts mechanical into electrical energy using a piezoelectric transducer. Some applications of PVEH have been proposed, including smart shoes [1,2], energy harvesting from walking vibration [3,4], and clothes and flexible plates made from piezoelectrical fiber materials [5,6]. To enhance harvesting efficiency, switch controls allow the reconfiguration of the harvesting circuit following some procedure, with multiple methods currently available [7-11]. Although synchronized switch energy harvesting on inductor (SSHI) has been proposed to control the switch device according to the vibration displacement [12–14], it requires external energy sources to drive a controller and external sensors to measure the vibration displacement. To realize a miniaturized and standalone harvester, switch-controlled PVEH with self-powered analog controllers and no external sensors has been achieved using different approaches. Lallart et al. [15] proposed a new self-powered architecture for optimized energy harvesting using piezoelectric elements with a low voltage output, as well as a theoretical development of harvested power taking into account non-linear effects introduced by discrete components. Chen et al. [16] proposed a velocity control synchronized switching circuit using three piezoelectric transducers that harvest electrical energy, supply electrical energy to a controller, and sense vibrational states of a structure, respectively. Lian and Liao [17] proposed a modified self-powered SSHI circuit improving conventional self-powered SSHI circuits that minimizes interference among different units in the circuit and removes resistive components. Chen et al. [18] discussed degradation of harvesting efficiency caused by switching delay and proposed an improved self-powered SSHI circuit. They replaced all components of a controller with equivalent impedance elements and discussed switching delays based on linear analysis. Liu et al. [19] also discussed degradation of harvesting efficiency caused by switching delays. They proposed a comprehensive model that is developed for improved performance analysis with missed factors included in comparison with previous investigations. Du et al. [20] proposed a new cold-startup SSHI interface circuit starting from cold start condition that dynamically increases the open-circuit voltage generated from the piezoelectric transducer in the cold state to start the system under much lower excitation levels. Wu et al. [21] proposed a piezoelectric energy harvesting circuit, which integrates a SSHI circuit and an active rectifier that ensures flipping of the piezoelectric voltage at optimal times and uses as a rectifier to further simplify the controller. Liu et al. [22] proposed an interface circuit for piezoelectric energy harvesting equipped with an active full bridge rectifier that was adopted to improve the power efficiency by reducing the conduction loss on the rectifying path. Self-powered PVEHs have been proposed besides SSHI. Wu et al. [23] and Shi et al. [24] proposed a self-powered synchronous electric charge excitation (SECE) circuit. SECE solves harvesting performance degradation due to failure in impedance matching. Makihara and Asahina [25] achieved an analog switching considering vibration suppression (SCVS) circuit with a controller that required neither a PC nor an outside power source. SCVS performs effective harvesting considering vibration-suppression effects. Analog controllers present switching delays that reduce the harvesting efficiency [18, 19, 26] and these neither expand to multimodal vibration nor change the control algorithm. In contrast, Yamamoto et al. [27] proposed a switch-controlled PVEH with a self-powered digital controller that can both expand to multimodal vibration structures and verify control methods.

In this study, we propose a measurement circuit to measure piezoelectric voltage. When the proposed measurement circuit is combined with a conventional switch-controlled PVEH with the self-powered digital controller [27], it can realize efficient harvesting in standalone. The resulting harvester improves miniaturization of the harvester compared with the conventional switch-controlled PVEH. As the objective of this study is proposing a novel measurement circuit in order for a digital controller equipped in a harvesting circuit to measure the piezoelectric voltage accurately, evaluation of the proposed harvester employs the fundamental switch control method. By rewriting the program of the digital controller, the proposed PVEH harvester can implement other sophisticated control methods. The proposed measurement circuit and the switch control to enhance harvesting efficiency are detailed in Section 2. The proposed circuit is evaluated through simulation and its harvesting efficiency is confirmed using the proposed harvester in Section 3. The proposed harvester has a comparable efficiency to conventional harvesters using external sensors. Finally, conclusions are drawn in Section 4.

2. Proposed method

2.1. Conventional switch control using external sensor

The piezoelectric voltage V_p given by Eq. (1) depends on the elongation and electric charge in a piezoelectric transducer [28]. Elongation of a piezoelectric transducer corresponds to the vibration displacement based on the assumption that the piezoelectric transducer is inserted between a base and a mass of a structure moving only along the vertical direction;

$$V_p = -b_p x + \frac{Q}{C_p}. \tag{1}$$

Here, b_p is a piezoelectric coefficient that is derived from a piezoelectric constant to represent a relationship between vibration displacement and voltage at a piezoelectric transducer.

Figure 1(a) shows a harvesting circuit with switch control. A piezoelectric transducer, rectifiers comprising diodes D_1 to D_4, a battery C_S, and a load resistor R_{load} are connected in parallel, conforming to the standard harvesting configuration, and a switch device S and an inductor L are also connected in parallel. The SSHI strategy is as follows. First, the state of the switch device is open. Subsequently, the switch device changes from the open to the closed state. The electric charge vibrates by the LC series resonance, resulting in the expression

$$L\ddot{Q}(t) + r\dot{Q}(t) + \frac{1}{C_p}Q(t) = b_p x_s. \tag{2}$$

The switch device changes its state after half the LC series resonance period, obtaining the electric charge

$$Q\left(\frac{\pi}{\omega_e}\right) = \gamma\left(Q_{before} - b_p C_p x_s\right)\left\{\cos\left(\sqrt{1-\zeta_e^2}\pi\right) + \frac{\zeta_e}{\sqrt{1-\zeta_e}}\sin\left(\sqrt{1-\zeta_e^2}\pi\right)\right\} + b_p C_p x_s, \tag{3}$$

where

$$\omega_e \equiv \frac{1}{\sqrt{LC_p}}, \quad \zeta_e \equiv \frac{r}{2}\sqrt{\frac{L}{C_p}}, \quad \gamma \equiv \exp\left(\frac{\pi r}{2}\sqrt{\frac{L}{C_p}}\right), \quad Q(0) = Q_{before}. \tag{4}$$

Here, we assume $\zeta_e \ll 1$ and $r = 0\ \Omega$. The resulting electric charge, Q_{after}, is expressed as

$$Q_{after} = -Q_{before} + 2b_p C_p x_s, \tag{5}$$

indicating that the sign of the electric charge is inverted, and its amplitude is increased compared to that before switching. As the piezoelectric voltage is raised up by the electric charge, the piezoelectric transducer with the large piezoelectric voltage by switching can supply more energy compared to standard harvesting. The largest increment in electric charge is obtained at maximum displacements x_s, which corresponds to the instant of zero velocity assuming sinusoidal vibration. A switch controller thus detects the instant that the structural velocity is zero. Figure 1(b) is a flowchart of the SSHI strategy and Fig. 1(c) is typical waveforms of vibration displacement, piezoelectric voltage and electric charge under SSHI strategy.

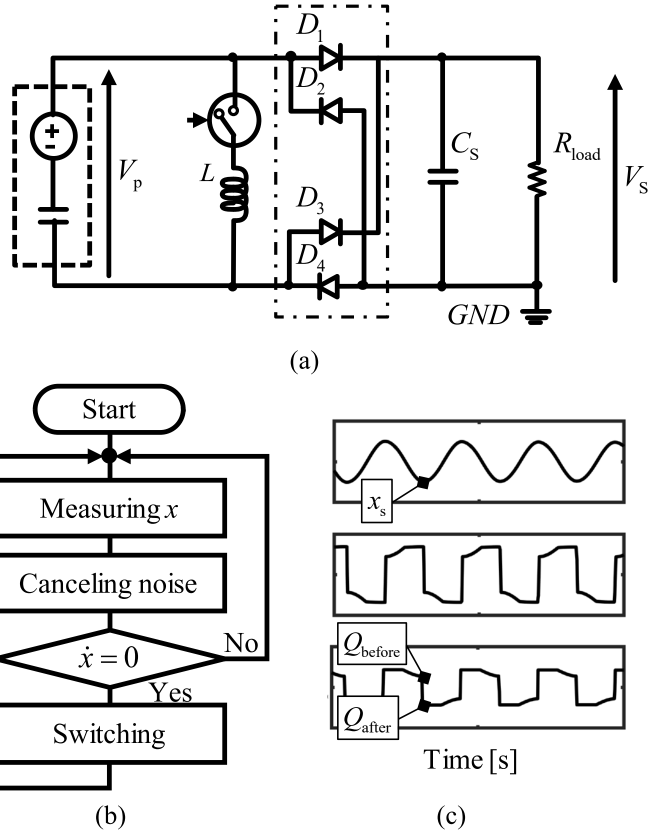

Fig. 1. (a) Circuit with switch control comprising switch S and inductance L. Rectifier composed of diodes D_1 to D_4 delivers a dc voltage to battery C_s and load R_{load}. (b) Flowchart of SSHI strategy. (c) Typical waveforms obtained from the SSHI strategy.

2.2. Modified SSHI strategy

A proposed switching strategy using piezoelectric voltage measurements, called modified SSHI strategy, is discussed. Figure 2(a) is a flowchart of the modified SSHI strategy. Figure 2(b) is typical waveforms of vibration displacement and velocity of the piezoelectric voltage dV_p/dt. In the proposed method, the switching is performed when the absolute value of the dV_p/dt becomes larger than a threshold. When the threshold is small, the switching is not performed accurately because of measurement noise. When the threshold is large, the switching delay problem occurs [17, 18, 25]. The switching law is written as

$$\text{If } \dot{V}_p[k] \text{ satisfy } \left|\frac{dV_p}{dt}[k-1]\right| < \varepsilon \text{ and } \left|\frac{dV_p}{dt}[k]\right| \geq \varepsilon, \text{ then switching,} \quad (6)$$

where k is discrete time and ε is the threshold value.

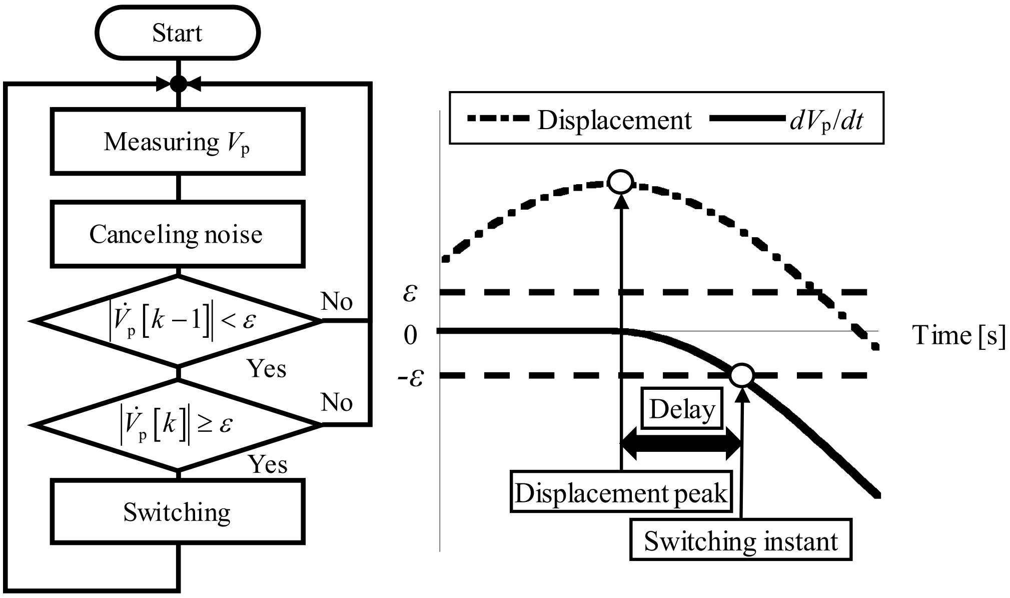

(a) (b)

Fig. 2. (a) Flowchart of modified SSHI strategy. (b) Typical waveforms of displacement and velocity of piezoelectric voltage.

2.3. Harvester with proposed measurement circuit

Figure 3 shows a proposed harvester including a measurement circuit. The harvester consists of three parts. First is the switch-controlled PVEH supplying energy to both the battery and load. Second is a self-powered digital controller comprising a calculator, an analog-to-digital convertor, and digital-to-analog convertor outputting the switch control signals according to the modified SSHI strategy. Third is a proposed measurement circuit measuring piezoelectric voltage based on differential measurement. The measured voltage is the difference between two measured signals:

$$V_{\mathrm{mes}} \equiv V_{\mathrm{pos}} - V_{\mathrm{neg}} \,. \tag{7}$$

The measured voltage and the piezoelectric voltage are in a proportional relationship.

The measurement circuit consists of six resistors R_1 to R_6 and has the following three features. First, the amplitude of measured signals is modified by the six resistors to ensure the measurable range, from 0 V to V_{drive}, of the analog-to-digital convertor in the digital controller. Because the amplitude of the piezoelectric voltage is much higher than the measurable range, the proposed circuit attenuates the piezoelectric voltage using the resistors. Specifically, the resistors R_1 to R_3 divide the positive piezoelectric voltage and the resistors R_4 to R_6 divide the negative piezoelectric voltage for delivering an appropriate voltage range to the convertor. Second, bias voltage is applied to the measured signals from the output of the dc-to-dc convertor to provide valid measurements for the digital controller. Both measured signals have negative values given by the forward voltage of the diodes. The digital controller considers 0 V whenever measured signals are below 0 V. It thus loses information of measured signals. Figures 4(a) and (b) show the waveforms of the measured signals with and without the bias voltage, respectively. As the digital controller cannot receive signals below 0 V, the measured signal without bias distorts the piezoelectric voltage measurement. Figure 4(c) confirms that the PVEH system with the self-powered digital controller receives a distorted differential measurement signal with invalid values below 0 V if no bias is applied. Third, electrical insulation is guaranteed by the diodes D_2 and D_4 to eliminate interference among the piezoelectric transducer and the digital controller.

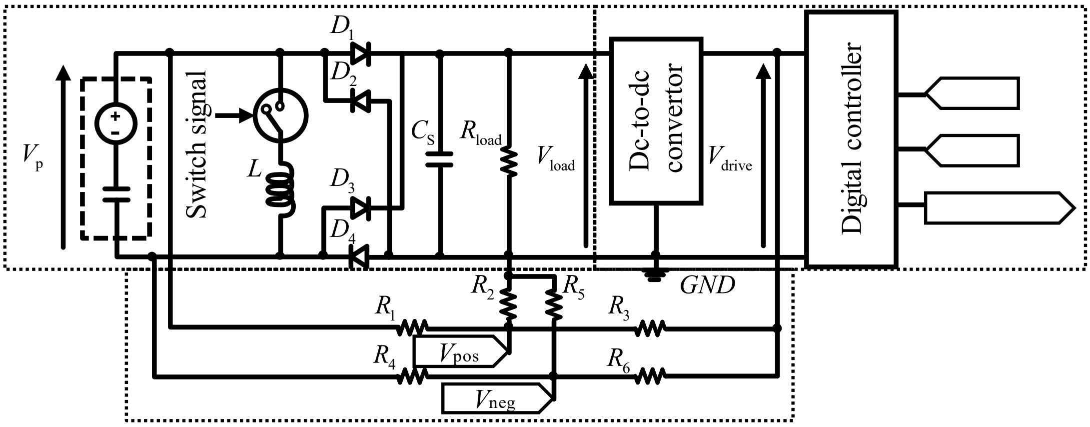

Fig. 3. Proposed harvester with measurement circuit and digital control.

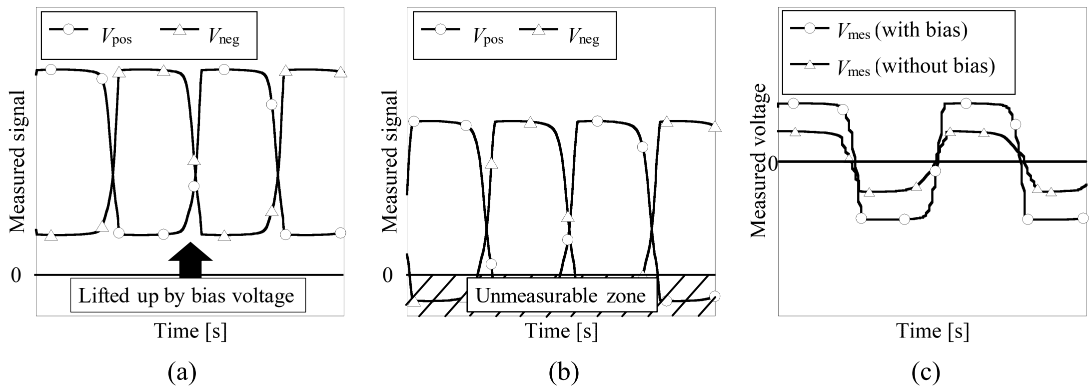

Fig. 4. Measured signals (a) with and (b) without bias voltage. (c) Comparison between biased and unbiased differential voltages.

3. Results and discussion

3.1. Simulations

The amplitudes of the measured signals can be determined by solving the circuit equation in steady state. When the piezoelectric transducer and the dc-to–dc convertor are considered as ideal voltage sources, the amplitudes of the measured signals are given by

$$V_{\mathrm{pos}} = \begin{cases} \dfrac{R_2R_3}{R_1R_2+R_1R_3+R_2R_3}V_{\mathrm{p}} + \dfrac{R_1R_2}{R_1R_2+R_1R_3+R_2R_3}V_{\mathrm{drive}} & \left(V_{\mathrm{p}} \geq 0\right) \\ \dfrac{R_1R_2}{R_1R_2+R_1R_3+R_2R_3}V_{\mathrm{drive}} & \left(V_{\mathrm{p}} < 0\right) \end{cases}, \tag{8}$$

$$V_{\mathrm{neg}} = \begin{cases} \dfrac{R_4R_5}{R_4R_5+R_4R_6+R_5R_6}V_{\mathrm{drive}} & \left(V_{\mathrm{p}} \geq 0\right) \\ \dfrac{R_5R_6}{R_4R_5+R_4R_6+R_5R_6}V_{\mathrm{p}} + \dfrac{R_4R_5}{R_4R_5+R_4R_6+R_5R_6}V_{\mathrm{drive}} & \left(V_{\mathrm{p}} < 0\right) \end{cases}. \tag{9}$$

Figure 5 is the proposed circuit in steady state, which is simulated on LTspice® XVII (Analog Devices, Inc., USA) using the parameters listed in Table 1. Figure 6 shows the simulation results for V_{p} and V_{mes}.

The measured voltage agrees with the piezoelectric voltage.

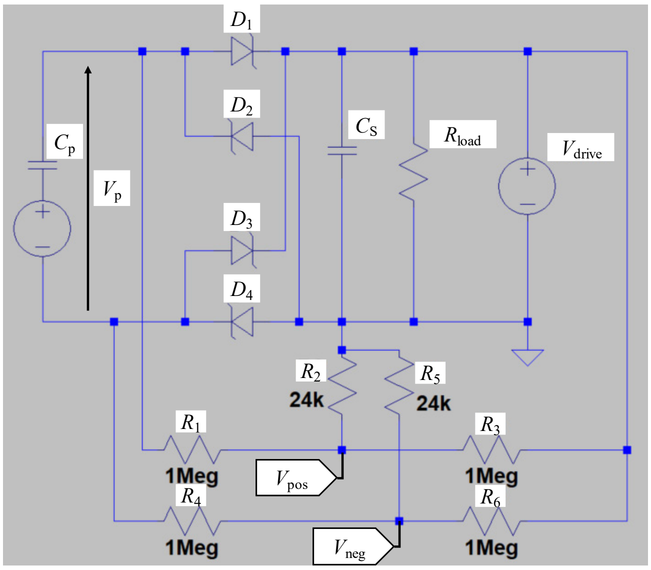

Fig. 5. Equivalent circuit in steady state simulated on the LTspice® XVII.

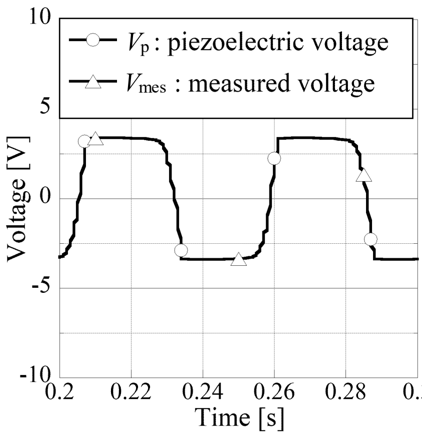

Fig. 6. Simulation results of the piezoelectric and measured voltages.

Table 1 Parameters of the electrical circuit for simulations and experiments.

Parameter	Symbol	Value	Unit
Piezoelectric coefficient	b_p	1.45×10^5	V/m
Transducer capacitance	C_p	6.61×10^{-7}	F
Dividing resistance	R_1, R_3, R_4, R_6	1.00×10^6	Ω
Dividing resistance	R_2, R_5	2.40×10^4	Ω
Inductance	L	2.00×10^{-2}	H
Load resistor	R_{load}	1.10×10^5	Ω
Battery capacitance	C_s	4.70×10^{-5}	F

3.2. Experimental setup

After confirming the circuit operation through simulations, the experiment was conducted shown in Fig. 7(a). The experimental two-degree-of-freedom vibration structure composes two masses and two springs, where mass 1 is vibrated by the oscillator in the vertical direction. The piezoelectric transducer is inserted between the base and mass 1. In this study, the structure is oscillated only in the first natural frequency of 18.7 Hz. The mechanical characteristics are listed in Table 2. Figure 7(b) shows the harvester connected to the piezoelectric transducer according to the diagram in Fig. 3.

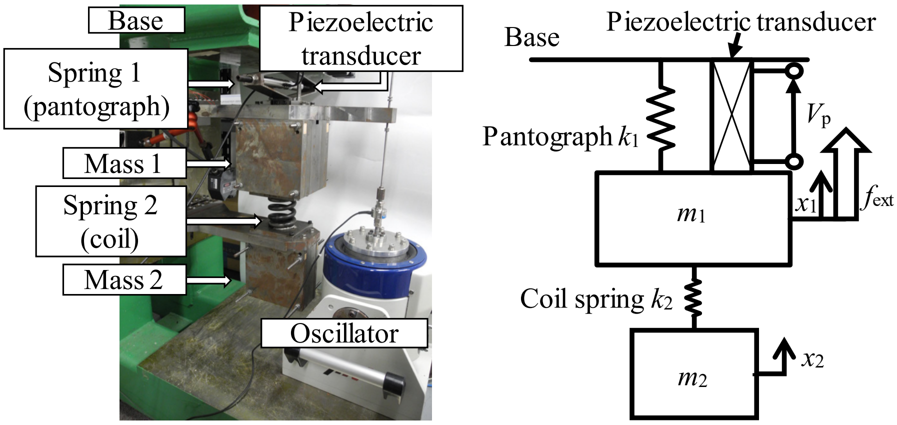

(a)

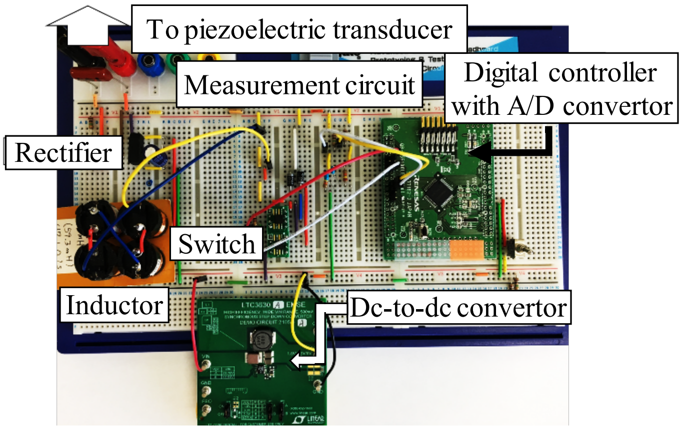

(b)

Fig. 7. (a) Two-degrees-of-freedom experimental structure combined with piezoelectric transducer. (b) Circuit of the proposed harvester implemented on a breadboard. (A/D, analog-to-digital)

Table 2 Mechanical characteristics of the experimental structure.

Parameter	Symbol	Value	Unit
Mass 1	m_1	3.24×10^1	kg
Mass 2	m_2	1.15×10^1	kg
Stiffness 1	k_1	1.17×10^6	N/m
Stiffness 2	k_2	2.09×10^5	N/m

3.3. Measuring test

First the proposed measurement circuit operation was evaluated, with results as shown in Figure 8. The top figure shows the displacement x_1. The middle figure shows the two signals V_{pos} and V_{neg} measured by the measurement circuit. The bottom figure shows the piezoelectric voltages measured by the external PC and the digital controller. The comparison of the two piezoelectric voltage signals shows that the measurement circuit is accurate.

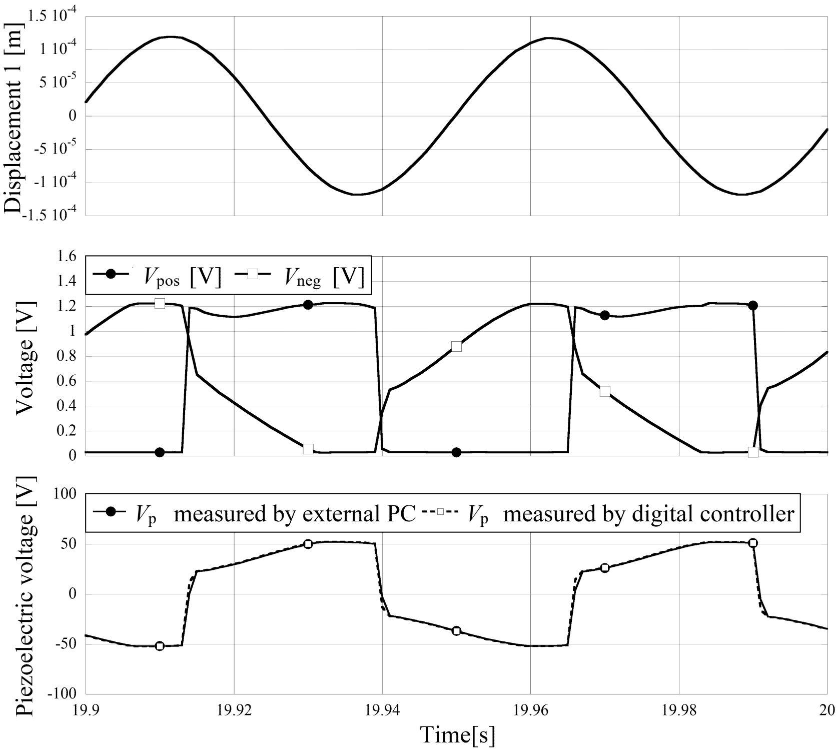

Fig. 8. Time history of displacement x_1, V_{pos}, V_{neg}, and V_p measured by external PC and digital controller.

3.4. Self-powered driving test

The internal consumption of the proposed circuit was evaluated. Table 3 shows the internal consumption of each component. The total internal consumption of the proposed circuit was 1.10 mW and the harvested power was 9.93 mW when the amplitude of the piezoelectric voltage was 25 V under open-circuit condition and the load resistor was 90 kΩ. The proposed harvester, which has a lower total internal consumption than harvested power, was driven by self-powering. The total power consumption of the resistors from R_1 to R_6, corresponding to the power consumption of the measurement circuit, was 0.064 mW. The power consumption of the digital controller was 0.097 mW. Table 4 shows the electronic components used in the proposed harvester.

Figure 9 shows the time history of the storage voltage and the piezoelectric voltage under cold-start conditions. The storage voltage reached a minimal driving voltage of the dc-to-dc convertor of 4.0 V at 0.7 s. Subsequently, the digital controller started at 1.7 s and the switching started at 2.0 s. The waiting time to avoid malfunctions was from 1.7 s to 2.0 s.

Table 3 Internal consumption in each component

Harvested power [mW]	Internal consumption [mW]	Component	Value [mW]
9.93	1.10	Measurement circuit (Resistors from R_1 to R_6)	0.064
		DC-to-dc convertor	0.148
		Analog-to-digital convertor (Sampling rate: 1 ms)	0.683
		Digital controller	0.097
		Switch device	0.110

Table 4 Electronic components used in the proposed harvester

Component	**Model number**	**Manufacturer**
Dc-to-dc convertor	LTC3630A	Linear Technology
Analog-to-digital convertor	RL78/G13	Renesas Electronics Corporation
Digital controller	RL78/G13	Renesas Electronics Corporation
Switch device	PS7205B-1A	NEC

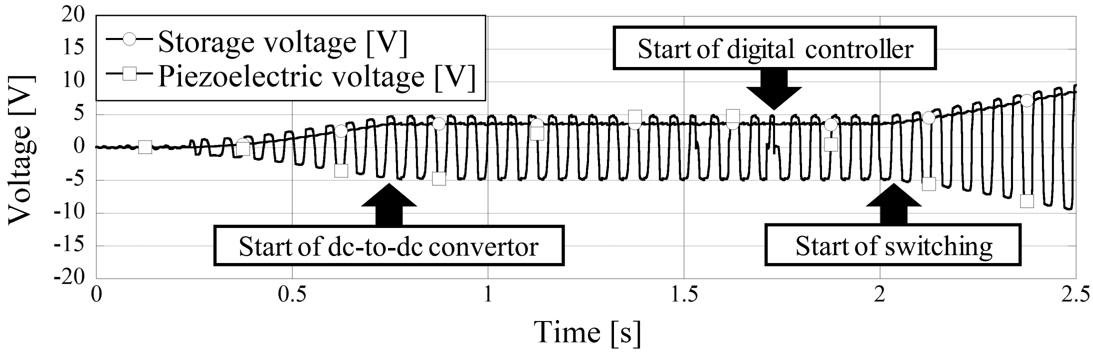

Fig. 9. Time history of storage voltage and piezoelectric voltage under cold-start condition.

3.5. Power harvesting evaluation

After verifying its operation, the harvesting performance of the proposed harvester was evaluated connecting a variable resistive load. The power delivered to the load resistor is given by

$$P_{\mathrm{load}} \equiv \frac{\left(V_{\mathrm{load}}\right)^2}{R_{\mathrm{load}}}. \tag{10}$$

Figure 10 shows the power consumption of the load resistor. The power consumption using any SSHI strategy was much higher than the standard harvesting for sufficiently high load resistors. The optimal resistance differed between the two SSHI cases and the standard harvesting case, as shown in Fig. 10. The internal impedance of PVEH is optimized based on the impedance matching theory. The internal impedance of the standard harvesting does not change because the standard harvesting keeps the switch open continuously. In contrast, the internal impedance of the SSHI changes frequently because the SSHI alters the state of the switch, and the inductor becomes activated while the state of the switch is closed. The optimal resistance of the SSHI corresponds to the average value per period of the internal impedance. The difference of the optimal resistances in each method depends on the difference of the internal impedance values caused by switching. Overall, the power supplied by the modified SSHI strategy was almost the same as that of the conventional sensor-equipped SSHI strategy. The difference between the modified and sensor-equipped SSHI was given by the proposed circuit and switching law. The proposed circuit consumed electrical energy at the resistance divisors. The modified SSHI had switching delays caused by the threshold ε in Eq. (6). The power consumption of the proposed circuit and the inappropriate switching of the modified SSHI strategy decreased the harvesting performance.

The power consumption was not evaluated in the range of the small load resistors in Fig. 10 because the digital controller did not function in self-powered in this region, which is referred to as a non-functional region. As most electrical current flew from the battery to the load resistor and little current flew from the battery to the dc-to-dc convertor, the dc-to-dc convertor and the digital controller were not driven by the harvested power in the non-functional region. Utilizing the proposed circuit in non-functional region was not supposed.

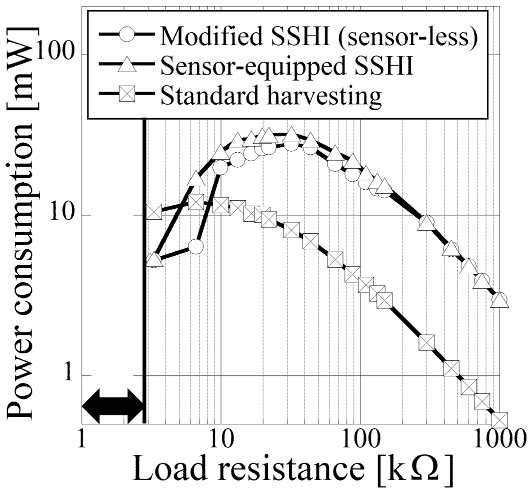

Fig. 10. Power consumption at load resistor using different approaches.

4. Conclusion

In this study, we proposed a novel measurement circuit to perform switch-controlled PVEH with a self-powered digital controller requiring no external sensors. The proposed circuit measures the piezoelectric voltage using differential measurement and has three main features. First, the circuit attenuates the amplitude of the piezoelectric voltage to the appropriate range for proper measuring of the self-powered digital controller. Second, the circuit performs conditioning on the measured signals using the bias voltage to allow suitable measuring by the digital controller. Third, the circuit suitably isolates the measured voltage from the measurement equipment. The proposed circuit accurately measured the piezoelectric voltage, which was used by the modified SSHI strategy to improve the harvesting efficiency. Furthermore, the power supplied by the proposed harvester was comparable to that by the conventional harvester equipped with a displacement sensor. The proposed harvester was superior to the conventional harvester in terms of compactness and autonomy, making it suitable for standalone portable devices.

Acknowledgments

This work was supported by a JSPS KAKENHI Grant-in-Aid for Scientific Research (B) (KAKENHI) (Grant Number JP18H01619) from the Japan Society for the Promotion of Science.

References

[1] L. Mateu, F. Moll, Appropriate charge control of the storage capacitor in a piezoelectric energy harvesting device for discontinuous load operation, Sens. Actuators A Phys. 132 (2006) 302–310. http://dx.doi.org/10.1016/j.sna.2006.06.061.

[2] N.S. Shenck, J.A. Paradiso, Energy scavenging with shoe-mounted piezoelectrics, IEEE Micro 21 (2001) 30–42. https://doi.org/10.1109/40.928763.

[3] J.M. Donelan, Q. Li, V. Naing, J.A. Hoffer, D.J. Weber, A.D. Kuo, Biomechanical energy harvesting: generating electricity during walking with minimal user effort, Science 319 (2008) 807–810. http://dx.doi.org/10.1126/science.1149860.

[4] L.C. Rome, L. Flynn, E.M. Goldman, T.D. Yoo, Generating electricity while walking with loads, Science 309 (2005) 1725–1728. http://dx.doi.org/10.1126/science.1111063.

[5] A. Delnavaz, J. Voix, Flexible piezoelectric energy harvesting from jaw movements, Smart Mater. Struct. 23 (2014) 105020. http://dx.doi.org/10.1088/0964-1726/23/10/105020.

[6] F. Narita, M. Fox, A review on piezoelectric, magnetostrictive, and magnetoelectric materials and

device technologies fro energy harvesting applications, Adv. Eng. Mater. 20 (2018) 1700743. http://dx.doi.org/10.1002/adem.201700743.

[7] K. Makihara, Y. Yamamoto, K. Yoshimizu, C. Horiguchi, H. Sakaguchi, K. Fujimoto, A novel controller to increase harvested energy from negating vibration-suppression effect, Smart Mater. Struct. 24 (2015) 037005. http://dx.doi.org/10.1088/0964-1726/24/3/037005.

[8] K. Yoshimizu, Y. Yamamoto, K. Asahina, K. Makihara, Strategy for enhancing the active harvesting of piezoelectric energy, J. Intell. Mater. Syst. Struct. 28 (2017) 1059–1070. http://dx.doi.org/10.1177/1045389X16672592.

[9] E. Lefeuvre, G. Sebald, D. Guyomar, M. Lallart, C. Richard, Materials, structures and power interfaces for efficient piezoelectric energy harvesting, J. Electroceram. 22 (2009) 171-179. http://dx.doi.org/10.1007/s10832-007-9361-6.

[10] S.-C. Kwon, J. Onoda, H.-U. Oh, Improvement of micro-jitter energy harvesting efficiency of piezoelectric-based surge-inducing optimal switching strategy, Sens. Actuators A Phys. 281, (2018) 55-66. https://doi.org/10.1016/j.sna.2018.08.043.

[11] H. Asanuma, K. Sakamoto, T. Komatsuzaki, Y. Iwata, Comparative study of electrical and switch-skipping mechanical switch for self-powered SSHI in medium coupled piezoelectric vibration energy harvesters, Smart Mater. Struct. 27 (2018) 075025. http://doi.org/10.1088/1361-665X/aac4cc.

[12] D. Guyomar, A. Badel, E. Lefeuvre, C. Richard, Toward energy harvesting using active materials and conversion improvement by nonlinear processing, IEEE Trans. Ultrason. Ferroelectr. Freq. Control 52 (2005) 584–595. http://dx.doi.org/10.1109/TUFFC.2005.1428041.

[13] A. Badel, D. Guyomar, E. Lefeuvre, C. Richard, Efficiency enhancement of a piezoelectric energy harvesting device in pulsed operation by synchronous charge inversion, J. Intell. Mater. Syst. Struct. 16 (2005) 889–901. http://dx.doi.org/10.1177/1045389X05053150.

[14] A. Badel, D. Guyomar, E. Lefeuvre, C. Richard, Piezoelectric energy harvesting using a synchronized switch technique, J. Intell. Mater. Syst. Struct. 17 (2006) 831–839. http://dx.doi.org/10.1177/1045389X06057533.

[15] M. Lallart, D. Guyomar, An optimized self-powered switching circuit for non-linear energy harvesting with low voltage output, Smart Mater. Struct. 17 (2008) 035030. http://dx.doi.org/10.1088/0964-1726/17/3/035030.

[16] Y.-Y. Chen, D. Vasic, F. Costa, W.-J. Wu, C.-K. Lee, A self-powered switching circuit for piezoelectric energy harvesting with velocity control, The Eur. Phys. J. Appl. Phys. 57 (2012) 30903. https://doi.org/10.1051/epjap/2012110355.

[17] J. Liang, W.-H. Liao, Improved design and analysis of self-powered synchronized switch interface circuit for piezoelectric energy harvesting systems, IEEE Trans. Ind. Electron. 59 (2012) 1950–1960. http://doi.org/10.1109/TIE.2011.2167116.

[18] Z. Chen, J. He, J. Liu, Y. Xiong, Switching delay in self-powered nonlinear piezoelectric vibration energy harvesting circuit: mechanism, effects and solution, IEEE Trans. Power Electron. 34 (2018) 2427–2440. http://doi.org/10.1109/TPEL.2018.2845701.

[19] W. Liu, A. Badel, F. Formosa, Q. Zhu, C. Zhao, G.-D. Hu, A comprehensive analysis and modeling of the self-powered synchronous switching harvesting circuit with electronic breakers, IEEE Trans. Ind. Electron. 65 (2018) 3899–3909. http://dx.doi.org/10.1109/TIE.2017.2762640.

[20] S. Du, G.A.J. Amaratunga, A.A. Seshia, A cold-startup SSHI rectifier for piezoelectric energy harvesters with increased open-circuit voltage, IEEE Trans. Power Electron. 34 (2018) 263–274. http://doi.org/10.1109/TPEL.2018.2815536.

[21] L. Wu, X.-D. Do, S.-G. Lee, D.S. Ha, A self-powered and optimal SSHI circuit integrated with an active rectifier for piezoelectric energy harvesting, IEEE Trans. Circuits and Syst. I: Reg. Papers. 64 (2017) 537–549. http://doi.org/10.1109/TCSI.2016.2608999.

[22] L. Liu, Y. Pang, W. Yuan, Z. Zhu, Y. Yang, A self-powered piezoelectric energy harvesting interface circuit with efficiency-enhanced P-SSHI rectifier, J. Semicond. 39 (2018) 045002. http://doi.org/10.1088/1674-4926/39/4/045002.
[23] Y. Wu, A. Badel, F. Formosa, W. Liu, A. Agbossou, Self-powered optimized synchronous electric charge extraction circuit for piezoelectric energy harvesting, J. Intell. Mater. Syst. Struct. 25 (2014) 2165–2176. http://doi.org/10.1177/1045389X13517315.
[24] G. Shi, Y. Xia, X. Wang, L. Qian, Y. Ye, Q. Li, An efficient self-powered piezoelectric energy harvesting CMOS interface circuit based on synchronous charge extraction technique, IEEE Trans. Circuits Syst. I: Reg. Papers. 65 (2018) 804–817. http://doi.org/10.1109/TCSI.2017.2731795.
[25] K. Makihara, K. Asahina, Analog self-powered harvester achieving switching pause control to increase harvested energy, Smart Mater. Struct. 26 (2017) 055007. http://dx.doi.org/10.1088/1361-665X/aa676c.
[26] M. Lallart, Y.-C. Wu, D. Guyomar, Switching delay effects on nonlinear piezoelectric energy harvesting techniques, IEEE Trans. Ind. Electron. 59 (2012) 464–472. http://dx.doi.org/10.1109/TIE.2011.2148675.
[27] Y. Yamamoto, K. Yoshimizu, K. Makihara, Synthetic assessment of self-powered energy-harvesting including robustness evaluation, JSME Mech. Eng. J. 2 (2015) 14-00549. http://dx.doi.org/10.1299/mej.14-00549.
[28] The Institute of Electrical and Electronics Engineers, IEEE Standard on Piezoelectricity 176-1987, (1987). https://doi.org/10.1109/IEEESTD.1988.79638.